Motion of Chips When Leaving the Cutting Zone during Chipboard Plane Milling

Pavel Rudak,[a] Štefan Barcík,[b] Mats Ekevad,[c] Oksana Rudak,[d] Marek Vančo,[e,*] and Jaroslava Štefková [f]

Mathematical equations were established and the following regularities of the plane milling process of wood materials were analyzed: effect of the cutting edge inclination angle on chip exit angle, influence of cutting edge inclination angle on speed of chip movement along the blade and exit speed of the chips from the cutting zone, dependence of the chip exit angle on the friction coefficients of the chips on the processed material surface and along the blade surface (friction coefficients were determined from the results of experimental measurements), and influence of mill rotation frequency on the chip exit angle. The milling of the chipboards with various mill designs was performed at different cutting parameters (diameter = 7 mm to 32 mm, number of cutting edges = 1 to 4, cutting edge inclination angle = -5° to 20°, frequency of mill rotation = 3000 min^{-1} to 24000 min^{-1}, feed per tooth = 0.1 mm to 1.5 mm). The process of chip exit from the cutting zone was photographed, and the chip exit angles were measured. A comparison of the chip exit angle values obtained from the experiments with those from the calculations based on the developed mathematical equations showed a high convergence.

Keywords: Milling; Wood material; Chipboard; Chips; Dust; Chip exit angle; Cutting edge; Inclination angle; Friction coefficient

Contact information: a: Belarusian State Technological University, Department of Material Science and Metal Technology, Forestry and Wood Technology Faculty, 13a, Sverdlova str., 220006, Minsk, Belarus; b: Technical University in Zvolen, Department of Machinery Control and Automation, Faculty of Environmental and Manufacturing Technology, 26, Studentska str., 960 53, Zvolen, Slovak Republic; c: Luleå University of Technology, Division of Wood Science and Engineering, Department of Engineering Sciences and Mathematics, 1, Forskargatan str., 931 87, Skelleftea, Sweden; d: Belarusian State Technological University, Department of Technology and Design of Wooden Articles, Forestry and Wood Technology Faculty, 13a, Sverdlova str., 220006, Minsk, Belarus; e: Technical University in Zvolen, Department of Environmental and Forestry Machinery, Faculty of Environmental and Manufacturing Technology, 26, Studentska str., 960 53, Zvolen, Slovak Republic; f: Technical University in Zvolen, Institute of Foreign Languages, Masarykova street 24, 960 53, Zvolen, Slovak Republic;
** Corresponding author: mvanco87@gmail.com*

INTRODUCTION

Wood materials, such as chipboard, wood fiberboard, medium-density fiberboard, *etc.*, are widely used in engineering. Milling is one of the most common cutting processes in woodworking (Gaff *et al.* 2015; Kvietková *et al.* 2015; Kubš *et al.* 2017). Computerized, numerically controlled (CNC) machines are most often used for the milling of wood materials. These machines can process the workpiece from different sides during a single setup on the machine. This technology provides high-quality processing performance and efficiency. At the same time, most industrial enterprises must deal with the problem of the

efficient removal of chips and dust from the cutting zone (Rudak and Kuis 2011; Rogoziński *et al*. 2015).

Woodworking mills operate at frequencies (n) of 3000 min^{-1} to 24000 min^{-1} and feed rates of 3 m/min to 40 m/min. Therefore, wood chips and dust have a high initial speed, which makes it difficult for the machine aspiration system to capture them (Nechepaev and Gnitko 2005; Pałubicki and Rogoziński 2016). The chips that are not caught by the aspiration system can fly up to 3 m to 5 m away from the processing zone. Such chips and dust mess the machine, workpieces, and surrounding space. When chips get into the area of the infrared sensors of a CNC machine, they can cause emergency stops and product defects. An inefficient chip exhaust from the cutting zone can cause an increased wear on the tools. Aspiration systems are used to create high-velocity air streams to collect chips and dust. At the same time they consume a large amount of electrical power, which results in increased costs (Wieloch *et al*. 2011).

One way to increase the efficiency of collecting chips from the cutting zone of milling machines is to use the kinetic energy of the chips and dust, which can direct their movement towards the chip receiver (Su and Wang 2002; Rudak and Kuis 2011). Manipulation of the chip motion in the required direction can be realized by the inclination of the tool blade. An inclined blade, especially one with helical edges, provides better chip flow compared with the conventional mill edge (Darmawan *et al.* 2011).

The cutting edge inclination angle has a major influence on the cutting process, durability of the tool, quality of the treated surface, and the cutting process costs (Pahlitzsch and Sommer 1966), as also mentioned in the previously conducted studies by the scientists from Technische Universität Dresden (Germany), Belarusian State Technological University (Belarus), Donetsk National Technical University (Ukraine), National Chiayi University (Taiwan), and Bogor Agricultural University (Indonesia). In these studies, the problem of chip exit from the cutting zone was affected to a limited extent. Understanding the process of chip and dust exit from the cutting zone is necessary to be able to use the kinetic energy of the chips and dust to improve the efficiency of their collection by the aspiration system (Barcík and Gašparík 2014; Kvietková *et al.* 2015).

The purpose of this study is to investigate the regularities of the movement of chips and dust particles when leaving the wood milling zone. To investigate the plane milling of the wood materials and establish equations describing the process of chip exit from the cutting zone, the following areas were focused on: 1) the effect of the cutting edge inclination angle on the chip exit angle, 2) influence of the cutting edge inclination angle on the chip movement speed along the cutting edge and chip exit speed from the cutting zone, 3) influence of the mill rotation frequency on the chip exit angle, and 4) comparison of the obtained experimental data with the results of the calculations conducted with the established equations.

EXPERIMENTAL

Materials

Chipboards with a double-sided laminate finish produced by EGGER Eurospan (Bucharest, Romania) were processed during the experiments. The thickness of the boards was 18 mm. The percentage of the binder was 10%, according to the product documentation. The average density of the plate, 670 kg/m^3, was found by weighing five

cubic cuts with the dimensions 18 mm × 18 mm × 18 mm from different sections of the plate.

Mills manufactured by the company Leitz GmbH & Co. KG (Oberkochen, Germany) were used in experiments.

Theory

A chip element with a mass of *m* located in the chip flute of the mill was considered for the mathematical modelling of the chip exit from the cutting zone. The tool has a radius of *R* and rotates with a cyclic frequency of ω. The wood material is milled at a milling depth of *e* (Fig. 1).

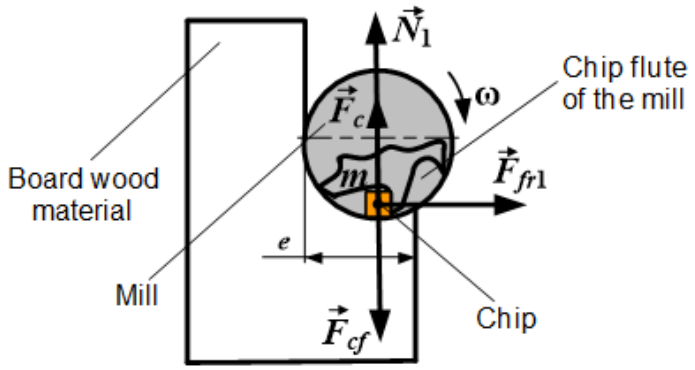

Fig. 1. A chip element located in the chip flute of the mill

The blade has a cutting edge inclination angle of λ (º). The chip element moves along the blade rectilinearly at a speed of V_x (m/s) (Fig. 2a). When the mill is rotated at an angle, ensuring the release of the chip flute, the chips leave at a speed of V_{exit} (m/s) and move at a chip exit angle of ν (º). The V_{exit} is the vector sum of the circular motion velocity (V_ω) (m/s) and V_x (m/s).

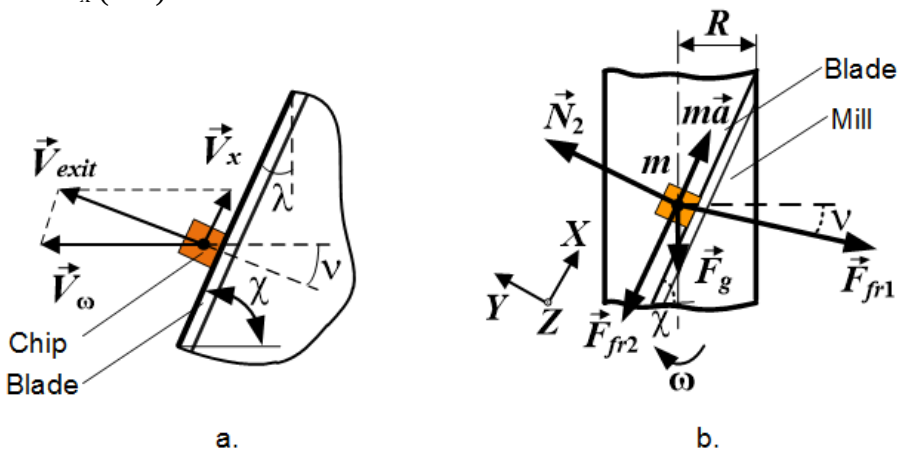

Fig. 2. Scheme of the (a) velocities at which the chip elements move and (b) forces acting on the chips in the chip flute of the mill

The motion of a chip particle was considered in the XYZ coordinate system, rotating together with the mill at a frequency of ω (rad/s). In this case, the X-axis was oriented parallel to the direction of the chip movement along the blade, and the Y-axis was

perpendicular to the indicated direction (Fig. 2b).

It was assumed that the chips were involved only in straight-line motion because the shape of the chips is very different from a sphere (Jamberová *et al.* 2016) and movement occurred over a short period of time.

Moving along the blade, the chip particle undergoes the action of the centrifugal force (F_{cf}), Coriolis force (F_c), and reaction of the processed material surface (N_1) (Fig. 1). The friction force (F_{fr1}) between the particle and processed material surfaces, gravitational force (F_g), and reaction force (N_2) of the blade surface also affect the chip particle movement (Fig. 2b).

The following equation of the equilibrium of forces acting on a chip particle was written, neglecting the aerodynamic and electrostatic forces and forces acting on a chip particle from other particles:

$$m\vec{a} = \vec{F}_g + \vec{F}_c + \vec{F}_{cf} + \vec{F}_{fr1} + \vec{F}_{fr2} + \vec{N}_1 + \vec{N}_2 \quad (1)$$

The auxiliary angle ($\chi = 90° - \lambda$) was introduced. Projection of the forces acting on the chip particle was performed on the axes coordinate. For the projections on the X-, Y-, and Z-axes, Eqs. 2, 3, and 4 were used, respectively:

$$ma_x = -F_{fr2} + F_{fr1}\cos(\nu + \chi) - mg\sin\chi \quad (2)$$

$$0 = N_2 - mg\cos\chi - F_{fr1}\sin(\nu + \chi) \quad (3)$$

$$0 = F_{cf} - F_c - N_1 \quad (4)$$

The friction force between the chip particle and processed material surface was determined by Eq. 5,

$$F_{fr1} = \mu_1 N_1 \quad (5)$$

where μ_1 is the friction coefficient between the chip particle and surface of the material being processed.

The friction force between the chip particle and blade surface was determined by the following equation,

$$F_{fr2} = \mu_2 N_2 \quad (6)$$

where μ_2 is the friction coefficient between the chip particle and blade surface.

Taking Eq. 4 into account, the equation to determine the friction force between the chip particle and surface of the material being processed was written as:

$$F_{fr1} = \mu_1 m\left(\omega^2 R - 2\omega V_x \cos\chi\right) \quad (7)$$

From Eq. 3, the following equation was obtained:

$$N_2 = \mu_1 m\left(\omega^2 R - 2\omega V_x \cos\chi\right)\sin\left(\nu + \chi\right) + mg\cos\chi \quad (8)$$

Taking into account Eqs. 2 and 7, and knowing the acceleration, the following differential equation was obtained:

$$\dot{V}_x = \mu_1\left(\omega^2 R - 2\omega V_x \cos\chi\right)\cos\left(\nu + \chi\right) - \mu_2\frac{N_2}{m} - g\sin\chi \quad (9)$$

From the vector sum of the velocities (Fig. 2a), Eq. 10 was generated:

$$\cos(\nu+\chi)=\frac{\omega R\cos\chi-V_x}{\sqrt{V_x^2+(\omega R)^2-2V_x\omega R\cos\chi}} \quad (10)$$

Equations 8 through 10 allowed for the analysis of the chip exit process from the cutting zone.

To solve the equations and design the graphical dependencies, the Math CAD computer program (Version 15, PTC Inc., Needham, MA, USA) was used. The chip mass was assumed to be 1 g.

Methods

The application of the developed mathematical model of the chip exit process from the cutting zone required the determination of μ_1 and μ_2 to calculate the chip exit angles during wood plane milling. The features of the wood cutting process are remarkable and unique because they cannot be completely recreated on test machines for the study of tribological characteristics by standard methods (*e.g.*, according to the scheme of reciprocating motion of contacting bodies on a tribometer). Thus, the friction coefficients need to be determined during the actual cutting process. These friction coefficients were determined by experiments using the described technique. The advantage of this technique was no need to use a tribometer. (Rudak and Kuis 2012; Rudak *et al.* 2012, 2015, 2016).

A dynamometer system was installed on a BIESSE ROVER B 4.35 CNC woodworking machine (Biesse S.P.A., Pesaro, Italy) with two working tables to measure the components of the cutting forces during chipboard plane milling (Fig. 3).

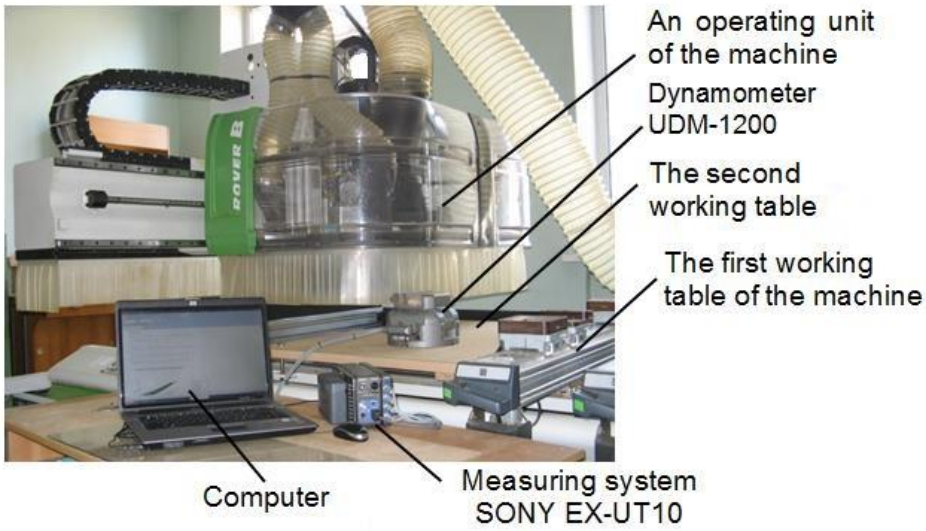

Fig. 3. Experiment setup with a dynamometer

First, the chipboard workpiece, which was machined by a mill, was fixed with the vacuum suckers of the first working table of the machine. The mill rotates about its axis and makes a feed motion with a speed of V_s.

A UDM-1200 dynamometer (All-Union Research Instrumental Institute, Moscow, Russia) was attached to the second working table of the machine. A second chipboard workpiece was fixed in the dynamometer to measure the cutting force components along

the direction of the mill feed (X_1-axis) and perpendicular to the feed direction (Z_1-axis). The workpieces on both work tables were installed end to end (Fig. 4).

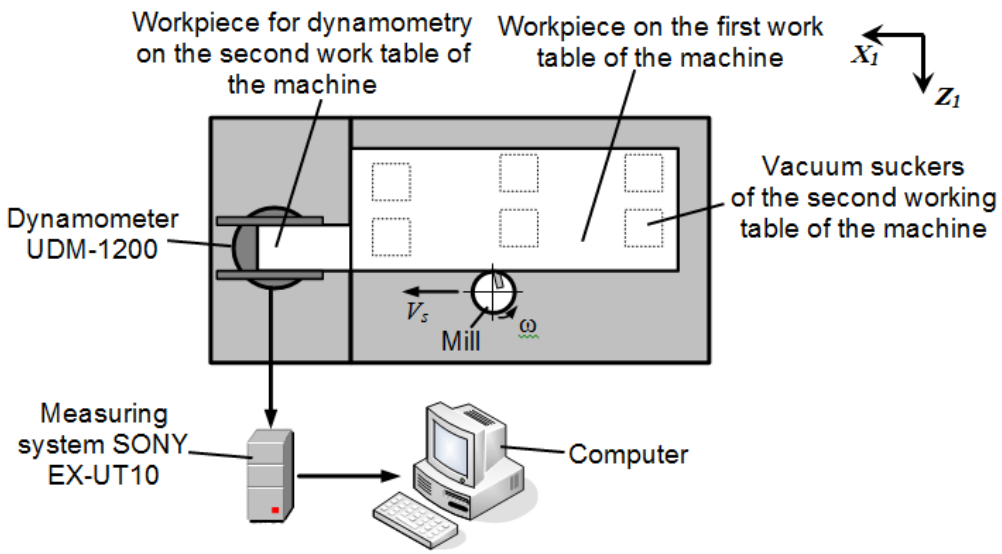

Fig. 4. Schematic diagram of the experiment setup for measuring the cutting force components

During the process of cutting the workpiece, the signal went from the dynamometer to a SONY EX-UT10 measuring system (Sony Corporation, Tokyo, Japan) and then to a personal computer, where it was processed (digital filtration) and visualized.

The average of the accumulated values was used (Vetterli *et al.* 2014) to process the signal from the measuring system. A TEKTRONIX TDS 2024B digital storage oscilloscope (Tektronix Inc., Beaverton, USA) was used.

The components of the cutting forces were determined to calculate the friction coefficients. Photographs of workpieces that were fixed on the work tables during the experiments to calculate the friction coefficients are shown in Fig. 5.

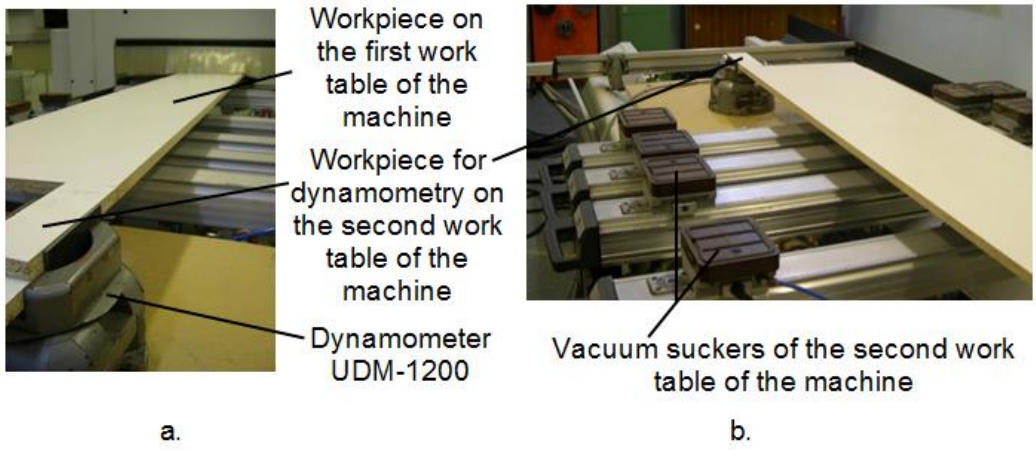

Fig. 5. Photographs from the (a) dynamometer side and (b) the side of the workpieces that were fixed on the work tables during the experiments to calculate the friction coefficients

The first work table was used for milling the workpiece at the cutting speed and chip thickness according to the methodology suggested by Rudak *et al.* (2016). This made it possible to reconstruct the temperature and other conditions during the real operation before dynamometry was performed.

The cutting forces were measured during milling the workpiece with the dynamometer on the second working table of the machine. A mill developed for this purpose was used to determine μ_1 (Karpovich *et al.* 2011). The diameter of the mill (d) was 32 mm and the number of cutting elements (z) was four. The developed mill could be used with and without a steel inner element (Fig. 6).

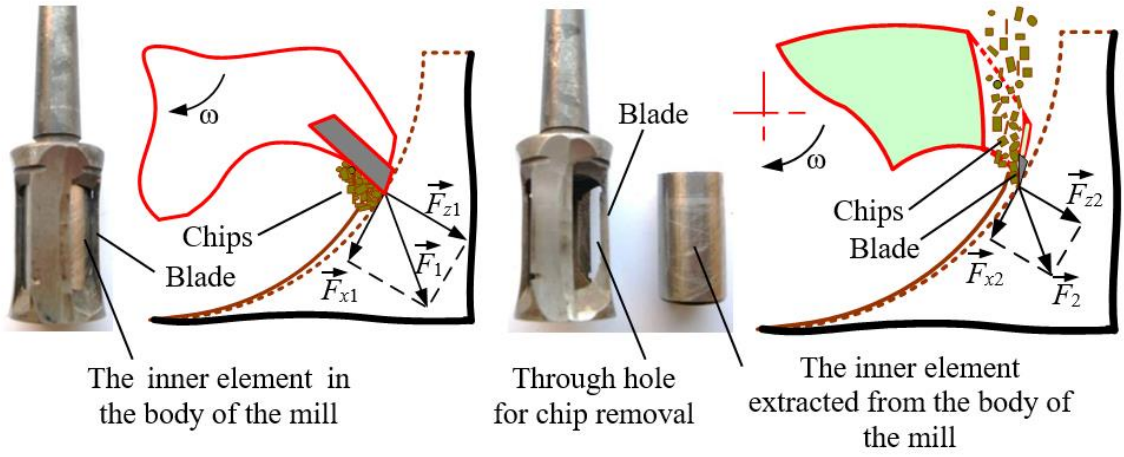

Fig. 6. Mill with an inner element for determination of μ_1: (a) the inner element installed in the body of the mill and (b) the inner element extracted from the body of the mill

The chips pass through the hole in the blade when the mill is operating without an inner element. This eliminates the contact of chips with the processed material surface.

The workpiece was first milled using a tool with an inner element. The tangential F_{x1} and radial F_{z1} components of the cutting force F_1 were determined in this case (Fig. 6a). Then, the workpiece was milled by a tool without the inner element. The tangential F_{x2} and radial F_{z2} components of the cutting force F_2 were determined in conditions with the absence of friction from the chips contacting the processed material surface (Fig. 6b).

The friction coefficient μ_1 was calculated according to Rudak (2012) and Rudak and Kuis (2012) with Eq. 11

$$\mu_1 = \frac{F_{x1} - F_{x2}}{F_{z1} - F_{z2}} \quad (11)$$

Mills with common designs were used to determine μ_2. The same mills were used for the experiments that determined the chip exit angles.

The tangent F_{xb} and normal F_{zb} components of the cutting force along the back surface of the blade were initially measured during milling with an e of 0. The cutting force components F_x (component of the cutting force in the feed direction) and F_z (component of the cutting force in a direction perpendicular to the feed direction) were measured further when the depth of the cut was removed (Fig. 7).

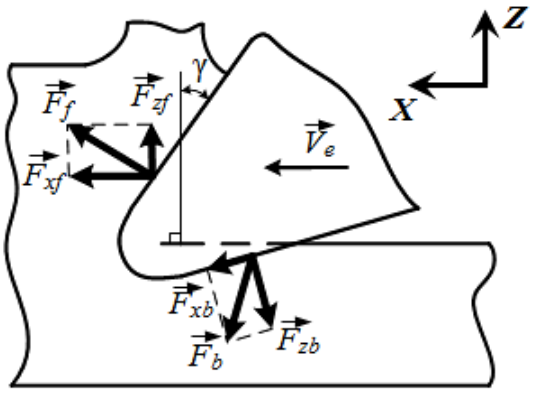

Fig. 7. Scheme of the forces acting on the blade surfaces (Bershadsky 1975)

The calculation of μ_2 was conducted according to Rudak *et al.* (2016) with Eq.12

$$\mu_2 = \mathrm{tg}(\gamma - \mathrm{arctg}(\frac{F_z - F_{zb}}{F_x - F_{xb}})) \quad (12)$$

where γ is the front angle of the blade (°).

The experimental studies were conducted on the woodworking machine A BIESSE ROVER B 4.35 (Biesse S.P.A., Pesaro, Italy) with CNC (Fig. 8).

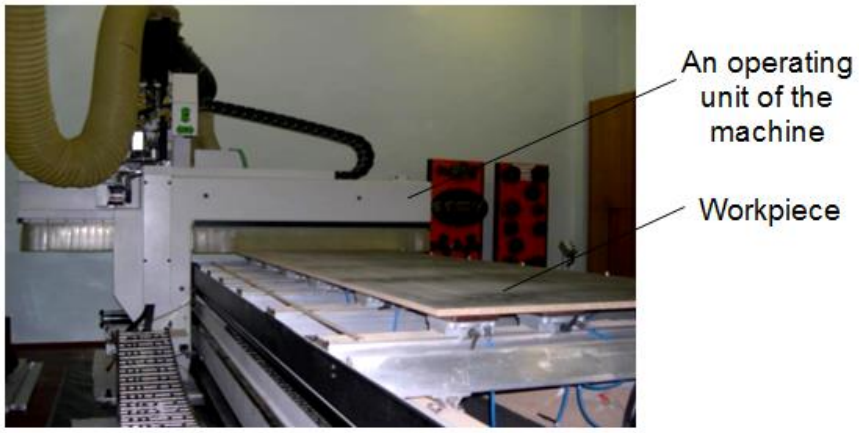

Fig. 8. Woodworking machine with a fixed workpiece

The milling of chipboards with various mill designs was performed at different cutting conditions (d = 7 mm to 24 mm, z = 1 to 3, λ = -5° to 20°, n = 3,000 min^{-1} to 24,000 min^{-1}, feed per tooth (S_z) = 0.1 mm to 1.5 mm).

The chip exit process from the cutting zone was recorded with a Nikon Coolpix L14 digital camera (Nikon Corporation, Tokyo, Japan). The photos were transferred to a personal computer where they were analyzed. The chip exit angles were measured in CAD Compass 3D v.12. (ASCON Group, St. Petersburg, Russia).

Figures 9 and 10 show examples of photos of the exit of chips and dust from the cutting zone.

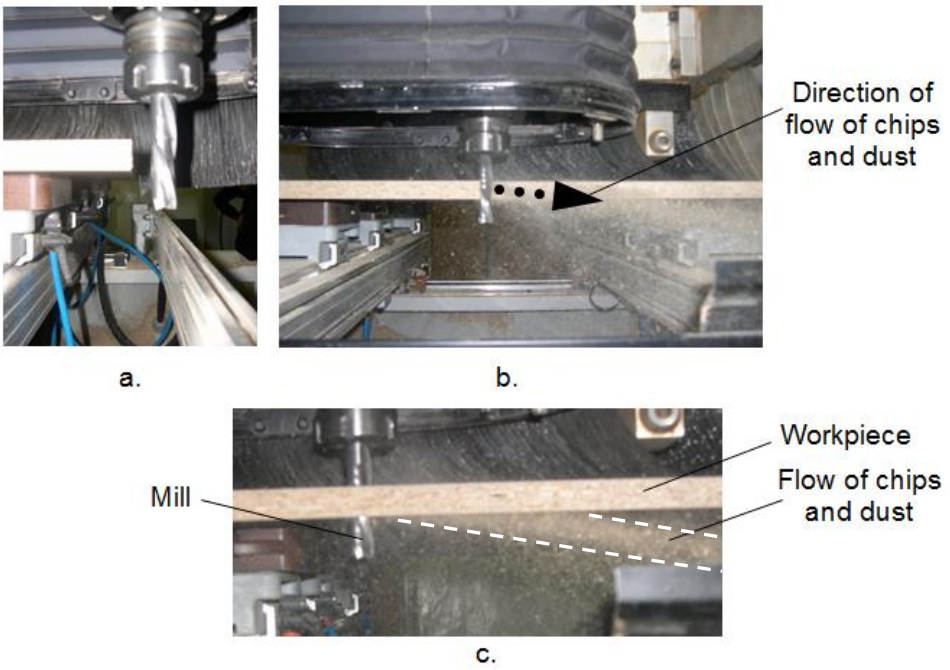

Fig. 9. One-piece tungsten-cobalt hard alloy mill (d = 16 mm, z = 2, and λ = -20°): (a) the spindle and the mill of the machine; and (b) exit of the chips and dust from the cutting zone during part-immersion milling (e = 5 mm < d) and (c) full-immersion milling (e = d)

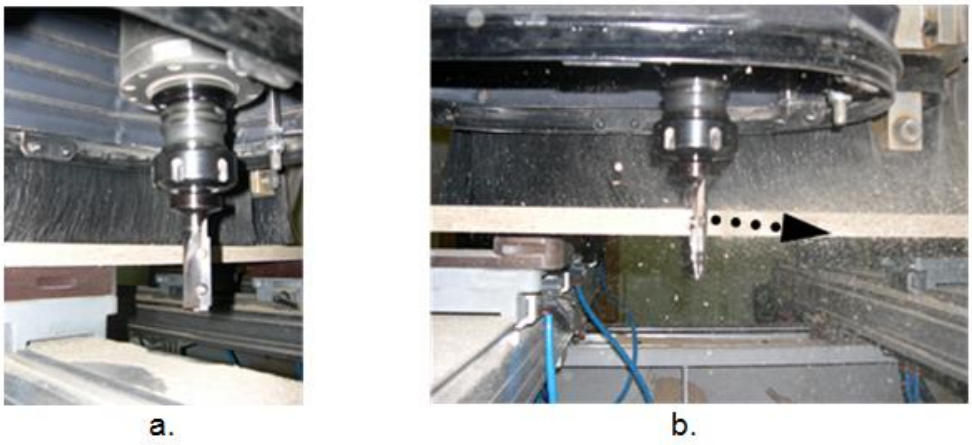

Fig. 10. (a) Indexable mill (d = 20 mm, z = 1, and λ = 0°) with replaceable inner elements from tungsten-cobalt hard alloy installed in the machine spindle, and (b) the chip and dust exit from the cutting zone at part-immersion milling (e = 5 mm < d)

RESULTS AND DISCUSSION

The solution of Eqs. 8 through 10 gave the following results. Figure 11 shows the dependence of v on λ (d = 20 mm, n = 24000 min^{-1}).

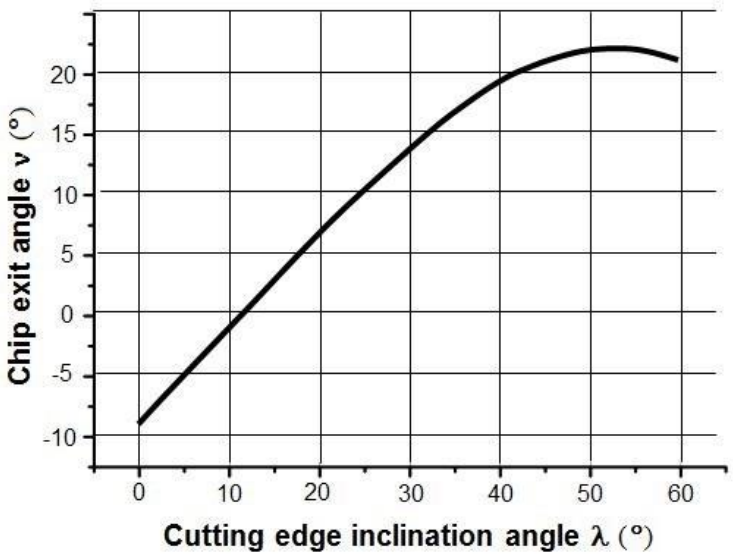

Fig. 11. Dependence of v on λ (d = 20 mm, n = 24000 min^{-1})

For λ values from 0° to 11.3°, the chips were directed downward when they exited. At λ of 11.3°, v was 0 and the chips left the cutting zone moving in a plane perpendicular to the axis of the mill rotation. With a further increase in λ, the chips left the cutting zone in an upwards direction. At λ of 25°, v was 10.4°. When λ was greater than 55°, v began to decrease.

Figure 12 shows the dependence of V_x of the chips along the blade and V_{exit} on λ (d = 20 mm, n = 24000 min^{-1}).

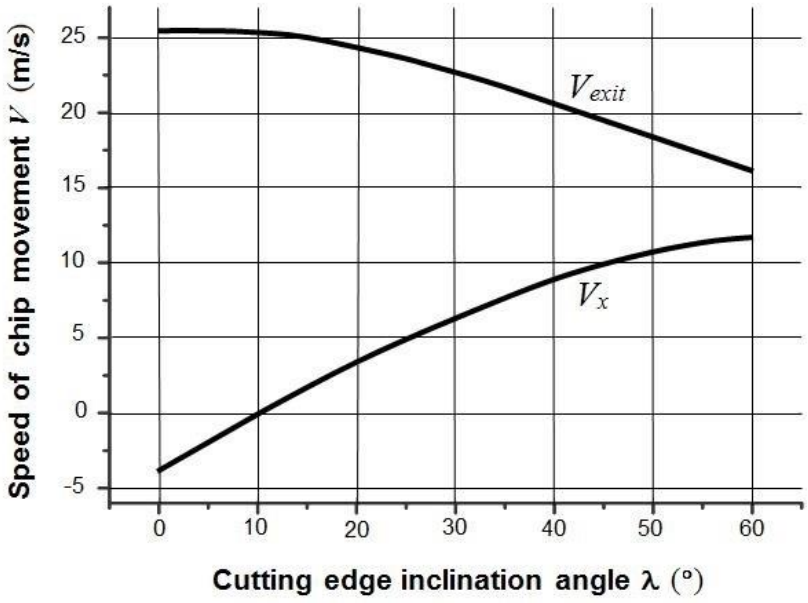

Fig. 12. Dependence of V_x of the chip movement along the blade and V_{exit} of the chips from the cutting zone on λ (d = 20 mm, n = 24000 min^{-1})

From Fig. 12, it can be seen that increasing the λ caused an increase in the V_x of the chip movement along the blade. The velocity vector V_x was directed along the blade and downwards for the λ values from 0° to 11.3°, which led to an unremarkable increase in the V_{exit}. A further increase in λ and V_x resulted in a decrease in the V_{exit}. Thus, V_{exit} increased when λ ranged from 0° to 55°. This was consistent with the results of the natural wood milling experiments. The flight speed of the chips decreased when the cutting edge inclination angle increased (Darmawan *et al.* 2011).

Figure 13 shows the dependence of v on μ_1 (at μ_2 = 0.2) and μ_2 (at μ_1 = 0.5) (d = 20 mm, λ = 25°). The figure shows that the values of μ_1 and μ_2 had a noticeable effect on the chip exit angle. This was consistent with the results from previous studies that showed a major effect of the blade tribological characteristics on the wood cutting process (Voskresenskiy 1955). The values of the friction coefficients obtained in this study agreed with the data reported in previous studies (McKenzie and Karpovich 1968; Xu *et al.* 2014; Yin *et al.* 2016). When μ_2 was more than 0.45, the chip exit angle acquired a negative value.

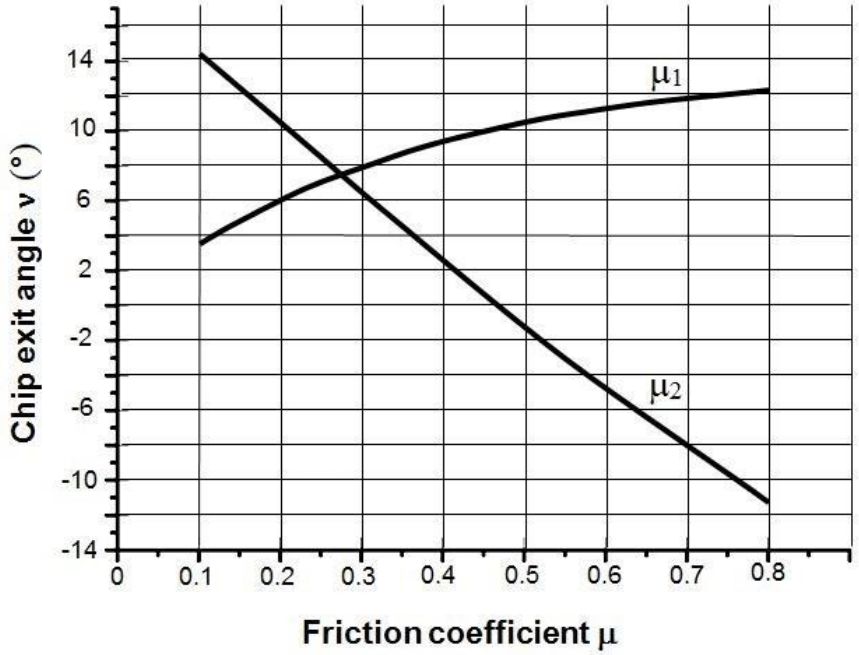

Fig. 13. Dependence of v on μ_1 (at μ_2 = 0.2) and μ_2 (at μ_1 = 0.5) (d = 20 mm, λ = 25°)

Figure 14 shows the dependence of v on the n (d = 20 mm, λ = 25°). At an n of 1000 min^{-1} and 3000 min^{-1}, v was 2.6° and 9.4°, respectively. With a further increase in the frequency of the mill rotation, the chip exit angle changed only slightly and remained at approximately 10°.

The conditions for carrying out the experiments to measure the components of the cutting forces in the chipboard plane milling process and the results of the calculation of μ_1 with the obtained data are presented in Table 1.

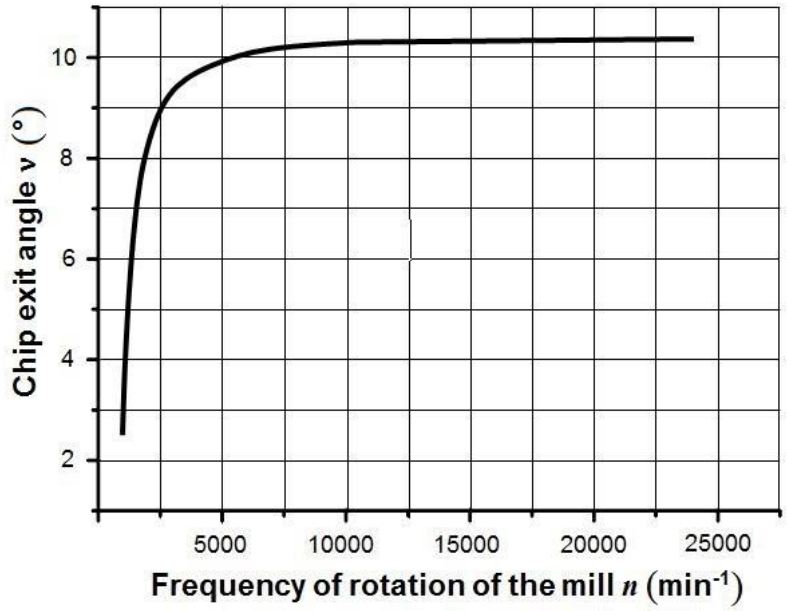

Fig. 14. Dependence of v on the n (d = 20 mm, λ = 25°)

Table 1. Conditions of the Experiments Measuring the Cutting Forces in the Chipboard Milling Process and Calculation of the Friction Coefficient (μ_1)

d (mm)	Type of Milling	S_z (mm)	e_{ave} (mm)	n (min^{-1})	V_s (m/min)	μ_1
32	Full-immersion	0.1	0.06	1300	0.52	0.52
	Down milling	0.2	0.03	3000	2.4	0.49
	Full-immersion	0.3	0.19	5250	6.3	0.46
	Full-immersion	0.4	0.25	12000	19.2	0.43
	Up milling	0.5	0.08	7500	15	0.41
	Down milling	1.0	0.16	11250	45	0.46
	Up milling	1.5	0.24	4500	27	0.43
	Full-immersion	0.25	0.16	10000	10	0.43
	Full-immersion	0.25	0.16	10000	10	0.46
	Full-immersion	0.25	0.16	10000	10	0.45
	Full-immersion	0.2	0.13	9000	7.2	0.52
	Up milling	0.2	0.03	12000	9.6	0.56
	Full-immersion	0.2	0.13	12000	9.6	0.49

e_{ave} – the average chip thickness; up milling – the mill rotates against the direction of the feed; down milling – the mill rotates with the direction of the feed

Table 2 presents the conditions and results of the experiments on the chip and dust exit process from the cutting zone and the results of calculating μ_2 during chipboard plane milling.

During the experiments to determine the chip exit angle and the process of full-immersion milling (the depth of the cut is equal to the diameter of the mill), it was found that the chips leaving the tool were formed into a dense stream (sheaf) by the walls of the groove in the processed material.

Table 2. Conditions and Results of the Experiments on the Chip and Dust Exit from the Cutting Zone and Results of Calculating the Friction Coefficient (μ_2)

d (mm)	z	λ (°)	Type of Milling	S_z (mm)	n (min^{-1})	μ_2	v (°)	v_{act} (°)
7	2	0	Full-immersion	0.1	2730	0.31	-14	-12
12	2	0	Down milling	0.2	1590	0.28	-12	-10
12	2	0	Full-immersion	0.3	1590	0.24	-10	-9
16	2	0	Full-immersion	0.4	1190	0.22	-9	-8
20	2	0	Up milling	0.5	1000	0.20	-8	-7
20	1	0	Down milling	1	1000	0.16	-7	-6
24	2	0	Up milling	1.5	1000	0.13	-6	-5
20	2	-5	Full-immersion	0.25	1000	0.19	-12	-10
20	2	0	Full-immersion	0.25	1000	0.18	-8	-9
20	2	5	Full-immersion	0.25	1000	0.21	5	4
12	2	20	Full-immersion	0.2	1590	0.18	8	10
16	2	20	Up milling	0.2	1190	0.22	6	8
16	3	-20	Full-immersion	0.2	1190	0.19	-23	-25

v_{act} – actual chip exit angle obtained from the experiments

Particles of chips and dust slowly lost their kinetic energy during full-immersion milling. Collecting the flow of chips and dust by increasing the speed of the air flow in the suction device requires high energy costs and is not effective. In this case, it is particularly advisable to use mills with a large cutting edge inclination angle to direct the flow of chips and dust towards the suction device.

In the case of part-immersion milling (the depth of the cut is smaller than the diameter of the cutter), the chips and dust left the cutting zone as a stream in the form of a wide fan, and the particles lost their kinetic energy faster than during full-immersion milling.

CONCLUSIONS

1. Mathematical dependencies were established that determined the chip exit angle, chip movement speed along the blade, and chip exit speed from the cutting zone, while taking into account the values of the cutting edge inclination angle, rotation frequency and radius of the mill, chip mass, and friction coefficients of the chips on the processed material surface and along the blade surface. These mathematical dependencies can be used when constructing wood-cutting mills and developing aspiration systems for wood-cutting machines. It is also possible to use the equations presented in this paper to find the optimal position of the machine suction device in the direction of the chip flow for the particular cutting conditions.
2. The greatest influence on the chip exit angle was from the cutting edge inclination angle. There was also a large influence on the chip exit angle from the friction coefficient of the chips along the blade surface and, to a somewhat lesser extent, the friction coefficient of the chips on the processed material surface. When the frequency of the mill rotation was more than 5000 min^{-1}, it did not affect the chip exit angle remarkably, but along with the mill radius, it determined the chip exit speed from the cutting zone and initial kinetic energy of the chips and dust.

3. The chip exit angles were determined based on the chipboard plane milling experiment. A high convergence was observed between the values of the chip exit angles obtained from the calculations with the established equations and results of the experiments.
4. It is advisable to apply a tool with a large cutting edge inclination angle to use the kinetic energy of the dust and chips to help the machine suction system collect them. This is especially effective for full-immersion milling, where the chips left the processing zone in the form of a dense stream of chips and dust that slowly lost their kinetic energy.
5. In the case of part-immersion milling, the chips and dust left the cutting zone as a stream in the form of a wide fan. The chips and dust lost their kinetic energy faster in such a scattered stream, which facilitated their collection by the aspiration system of the machine.

ACKNOWLEDGMENTS

This work and paper were funded by the Belarusian Republican Foundation for Fundamental Research (project TM12-098; "Develop an energy-saving system for efficient waste removal from the cutting zone of milling woodworking machines") and the Scientific Grant Agency of the Ministry of Education, Science, Research and Sport of the Slovak Republic and Slovak Academy of Sciences (project VEGA 1/0315/17; "Research of relevant properties of thermally modified wood at contact effects in the machining process with the prediction of obtaining an optimal surface", and project VEGA 1/0725/16; "Prediction of the quality of the generated surface during milling solid wood by razor endmills using *CNC* milling machines").

REFERENCES CITED

Barcík, Š., and Gašparík, M. (2014). "Effect of tool and milling parameters on the size distribution of splinters of planed native and thermally modified beech wood," *BioResources* 9(1), 2014, 1346-1360. DOI: 10.15376/biores.9.1.1346-1360

Bershadsky, A. L. (1975). *Резание древесины* [*Wood cutting*], Vishejshaja skola, Minsk, Belarus.

Darmawan, W., Gottlöber, C., Oertel, M., Wagenführ, A., and Fischer, R. (2011). "Performance of helical edge milling cutters in planing wood," *European Journal of Wood and Wood Products* 69(4), 565-572. DOI: 10.1007/s00107-010-0517-8

Gaff, M., Kvietková, M., Gašparík, M., Kaplan, L., and Barcík, Š. (2015). "Effect of selected parameters on the surface waviness in plane milling of thermally modified birch wood," *BioResources* 10(4), 7618-7626. DOI: 10.15376/biores.10.4.6512-6521

Jamberová, Z., Vančo, M., Barcík, S., Gaff, M., Čekovská, H., Kubš, J., and Kaplan, L. (2016). "Influence of processing factors and species of wood on granulometric composition of juvenile poplar wood chips," *BioResources* 11(4), 9572-9583. DOI: 10.15376/biores.11.4.9572-9583

Karpovich, S., Sambuk, P., Rudak, P., and Lukash, V. (2011). "Фреза контурная [The contour mill]," Republic of Belarus Patent No. 7616.

Kvietková, M., Barcík, Š., and Aláč, P. (2015). "Impact of angle geometry of tool on

granulometric composition of particles during the flat milling of thermally modified beech," *Wood Research* 60(1), 137-146.

Kvietková, M., Gašparík, M., and Gaff, M. (2015). "Effect of thermal treatment on surface quality of beech wood after plane milling," *BioResources* 10(3), 4226-4238, DOI: 10.15376/biores.10.3.4226-4238

Kubš, J., Gašparík, M., Gaff, M., Kaplan, L., Čekovská, H., Ježek, J., and Štícha, V. (2017). "Influence of thermal treatment on power consumption during plain milling of lodgepole pine (*Pinus contorta* subsp. Murrayana)," *BioResources* 12(1), 407-418, DOI: 10.15376/biores.12.1.407-418

Pahlitzsch, G., and Sommer, I. (1966). "Production of wood chips with a cylinder-type chipping-machine – Part III: Effect of inclination angle, knife-edge angle and cut direction angle," *Holz Roh. Werkst.* 24(4), 158-166. DOI: 10.1007/BF0260808

McKenzie, W., and Karpovich, H. (1968). "The frictional behaviour of wood," *Wood Sci. Technol.* 2(2), 139-152. DOI: 10.1007/BF00394962

Nechepaev, V., and Gnitko, A. (2005). "Системный подход к проектированию устройств удаления стружки при фрезеровании закрытых профильных пазов [A systematic approach to the design of chip removal devices when milling closed profile grooves]," *Reliability of the Instrument and Optimization of Technological Systems: A Collection of Scientific Works* 17, 302-307.

Pałubicki, B., and Rogoziński, T. (2016). "Efficiency of chips removal during CNC machining of particleboard," *Wood Research* 61(5), 811-818.

Rogoziński, T., Wilkowski, J., Górski, J., Czarniak, P., Podziewski, P., and Szymanowski, K. (2015). "Dust creation in CNC drilling of wood composites," *BioResources* 10(2), 3657-3665. DOI: 10.15376/biores.10.2.3657-3665

Rudak, P., and Kuis, D. (2010). "Эффективное удаление стружки и пыли из области обработки в процессе фрезерования древесных материалов [Effective removal of chips and dust from the processing area during the milling of wood materials]," in: *Resource- and Energy-Saving Technologies and Equipment, Environmentally Safe Technologies: Materials of International Scientific-Technical Conference*, Minsk, Belarus, pp. 121-124.

Rudak, P., and Kuis, D. (2011). "Снижение шумовых характеристик и повышение эффективности удаления стружки из зоны резания при эксплуатации дереворежущих машин [Reducing noise characteristics and increasing the efficiency of chip removal from the cutting zone when operating wood-cutting machines]," *Proceedings of BSTU* 2, pp. 245-247.

Rudak, P., and Kuis, D. (2012). "Триботехнические испытания твердосплавных неперетачиваемых режущих пластин с покрытиями при цилиндрическом фрезеровании древесностружечных плит [Tribotechnical tests of hard-alloy non-resharpened cutting elements with coatings for cylindrical milling of chipboards]," in: *Woodworking: Technologies, Equipment, Management of the XXI Century: The Proceedings of the VII International Eurasian Symposium*, Yekaterinburg, Russia, pp. 154-159.

Rudak, P., Kuis, D., and Rudak, O. (2012). "Методика триботехнических испытаний инструмента при фрезеровании древесностружечных плит [Technique of tribotechnical testing of tools for milling wood chipboards]," in: *New Materials, Equipment and Technologies in Industry: A Collection of Materials of the International Scientific and Technical Conference of Young Scientists*, Mogilev,

Belarus, pp. 82.

Rudak, P., Kovač, J., Kuis, D., Rudak, O., Barcík, Š., Krilek, J., and Razumov, E. (2015). "Experimental researches tribological properties of hard-alloy blades with a vacuum-plasma coating in the chipboards milling process," *Acta Universitatis Agriculturae et Silviculturae Mendelianae Brunensis* 63, 1543-1547. DOI: 10.11118/actaun201563051543

Rudak, P., Kuis, D., Rudak, O., and Piskunova, O. (2016). "Способ определения коэффициента трения по задней поверхности лезвия с режущей кромкой и коэффициента трения по передней поверхности лезвия при фрезеровании древесно-плитных материалов: патент Респ. Беларусь [Method for determining the coefficient of friction along the back surface of a blade with a cutting edge and the coefficient of friction along the front surface of the blade when milling wood-plate materials]," Republic of Belarus Patent No. 20337.

Su, W.-C., and Wang, Y. (2002). "Effect of the helix angle of router bits on chip formation and energy consumption during milling of solid wood," *Journal of Wood Science* 48(2), 126-131. DOI: 10.1007/BF00767289

Vetterli, M., Kovačević, J., and Goyal, V. (2014). *Foundations of Signal Processing*, Cambridge University Press, Cambridge, UK.

Voskresenskiy, S. (1955). *Резание древесины* [*Wood Cutting*], Goslesbumizdat, Moscow, Russia.

Wieloch, G., Pichit, S., and Barcik, S. (2011). "Tool dedusting system DFC by Leitz," in: *Proceedings of the 4th International Science Conference Woodworking Techniques*, Prague, Czech Republic, pp. 362-369.

Xu, M., Li, L., Wang, M., and Luo, B. (2014). "Effects of surface roughness and wood grain on the friction coefficient of wooden materials for wood-wood frictional pair," *Tribol. T.* 57(5), 871-878. DOI: 10.1080/10402004.2014.920064

Yin, W., Liu, Z., Tian, P., Tao, D., Meng, Y., Han, Z., and Tian, Y. (2016). "Tribological properties of wood as a cellular fiber-reinforced composite," *Biotribology* 5, 67-73. DOI: 10.1016/j.biotri.2015.09.005

Article submitted: July 21, 2017; Peer review completed: September 10, 2017; Revised version received: November 18, 2017; Accepted: November 19, 2017; Published: November 29, 2017.
DOI: 10.15376/biores.13.1.646-661